TAO, Vol. 9, No. 3, 363-378, September 1998

Deformation of the Philippine Sea Plate Under the Coastal Range, Taiwan: Results From an Offshore-Onshore Seismic Experiment

Eric A. Hetland[1] and Francis T. Wu[1]

(Manuscript received 21 January 1998, in final form 24 June 1998)

ABSTRACT

The ongoing orogeny in Taiwan is a result of the collision of the Philippine Sea and the Eurasian plates. While the structure of the continental crust on the Eurasian plate (EP) is now mostly known, that of the oceanic crust on the Philippine Sea plate (PSP) is not well mapped. Using offshore-onshore refraction data, collected during the R/V Ewing cruise of 1995, we investigate the nature of the transition between the EP and the PSP in the vicinity of the southern Coastal Range of Taiwan. The data were produced by the air-gun array of the R/V Ewing along a WNW-ESE trending line off the coast of central Taiwan (MCS/OBS line 23). The refracted P waves were collected by 19 RefTek recorders with L-28 sensors placed along the southern cross-island highway of Taiwan, which is the onshore extension of line 23. Because of high noise levels in the Coastal Plain, we were only able to retrieve usable data from 11 stations located from the east coast through the Central Range. We performed forward modeling of the first arriving waves at these stations; our strategy was to search for the simplest model that fitted all the data. Our results indicate that the crust thickens gradually toward Taiwan, from about 9-12 km thick in the Huatung basin to 15-18 km thick off the eastern coast of Taiwan, with a 4-8 degree dip of the Moho. Continuing westward, the crust thickens more rapidly to 27-32 km thick under the east coast of Taiwan, with a 26-32 degree dip of the Moho.

(Key words: Onshore/offshore seismic refraction, Arc-continent collision, Crustal thickening, Orogeny)

1. INTRODUCTION

It is commonly recognized that Taiwan was created as the former Luzon volcanic arc collided with the Eurasian continental shelf (Biq, 1972; Chai, 1972). But the timing of the various collision events and the mechanisms and nature of the collisions are continually being explored (e.g., Biq, 1981; Suppe, 1987; Davis *et al.*, 1983; Teng, 1990, 1996; Wu *et al.*, 1997).

[1] Department of Geological Sciences, State University of New York at Binghamton, Binghamton, NY 13902, USA

While the evolution of the orogeny can be constructed from geological mapping, the mechanical modeling has to include the three dimensional features of the orogen. Two main hypotheses have been proposed regarding the mechanics of the orogeny. On the one hand, the "thin-skinned" hypothesis (Suppe, 1987) views the building of the Central Range of Taiwan as a result of the westward overthrust of the Philippine Sea plate (PSP) onto the Eurasian plate (EP). In this model, the mountains are built entirely out of Tertiary sediments, with the PSP acting as a "rigid indenter" or a "bulldozer" and the EP subducting underneath the PSP (Davis *et al.*, 1983). On the other hand, the "lithospheric collision" model (Wu *et al.*, 1997) proposed that the entire lithospheres of the PSP and EP are in collision, and thus shortening and deformation should occur in both the PSP and EP.

The deformation associated with the collisional mountain building has been studied mostly on the basis of onshore geophysical and geological surveys (e.g., Ho, 1986; Wu, 1978; Suppe, 1981, 1987). Although marine surveys around the island have been conducted since the early 1970's (e.g., Bowin *et al.*, 1978), the deep crustal structures have not been mapped. It is evident that the structure of the oceanic crust in the vicinity of the collision can provide a strong constraint for modeling the collision. The crustal thickness represents an integrated effect of the deformation since the collision began, and its changes allow us to determine the crustal response of the PSP in the collision. In the common depiction of the thin-skinned model, the oceanic lithosphere should overlie the continental upper-crust of the EP. Alternatively, the PSP could be considered rigid and therefore the crustal thickness would remain unchanged. Tomography using the earthquake data recorded by the Taiwan Seismic Network has already shown the presence of a root and the relatively high velocity rocks at shallow depths under the Central Range (Rau and Wu, 1995; Rau 1996). Based on these and other observations, Wu *et al.* (1997) concluded that the thin-skinned hypothesis is inadequate in the modeling of Taiwan, and, in its stead, proposed the lithospheric collision model.

The marine-based data east of Taiwan can be used to further test the newly proposed model as well as the thin-skinned model. In particular, the data gathered during the 1995 R/V Ewing (cruise EW9509) offshore-onshore experiment (Figure 1), provide new information on the crustal structure of the PSP and the transition zone near Taiwan. The seismic waves from the air-gun shots were recorded up to offsets of about 200 km. A preliminary model of OBS line 23 by Wang *et al.* (1996) showed a gradually thickening of the crust from the Huatung Basin toward Taiwan. The OBS-airgun geometry yielded essentially split profiles along the line and could be modeled with little difficulty. However, since the profile stops short of the Taiwan coast, it does not cover the transition zone where changes in crustal structure are likely to be most rapid. On the other hand, the onshore stations recorded waves crossing this transition. Preliminary analyses (Hetland and Wu, 1996, 1997; Shih *et al.*, 1996, 1997; Lin *et al.*, 1997) of these data show that their quality is sufficient to resolve several important features in the crust. Our present study is a more detailed analysis of the southern onshore profile, along the extension of MCS/OBS line 23 (Figure 1). The onshore extension lies in the middle of the main collision zone of Taiwan, roughly between 22°N and 23.5°N. It is in this section that orogenic activity is the most active (Wu *et al.*, 1997). The eastern end of our onshore line is the Coastal Range, which is separated from the Central Range by the Longitudinal Valley (LV; Figure 1). The LV is evidently the contact between the EP and the PSP at the surface

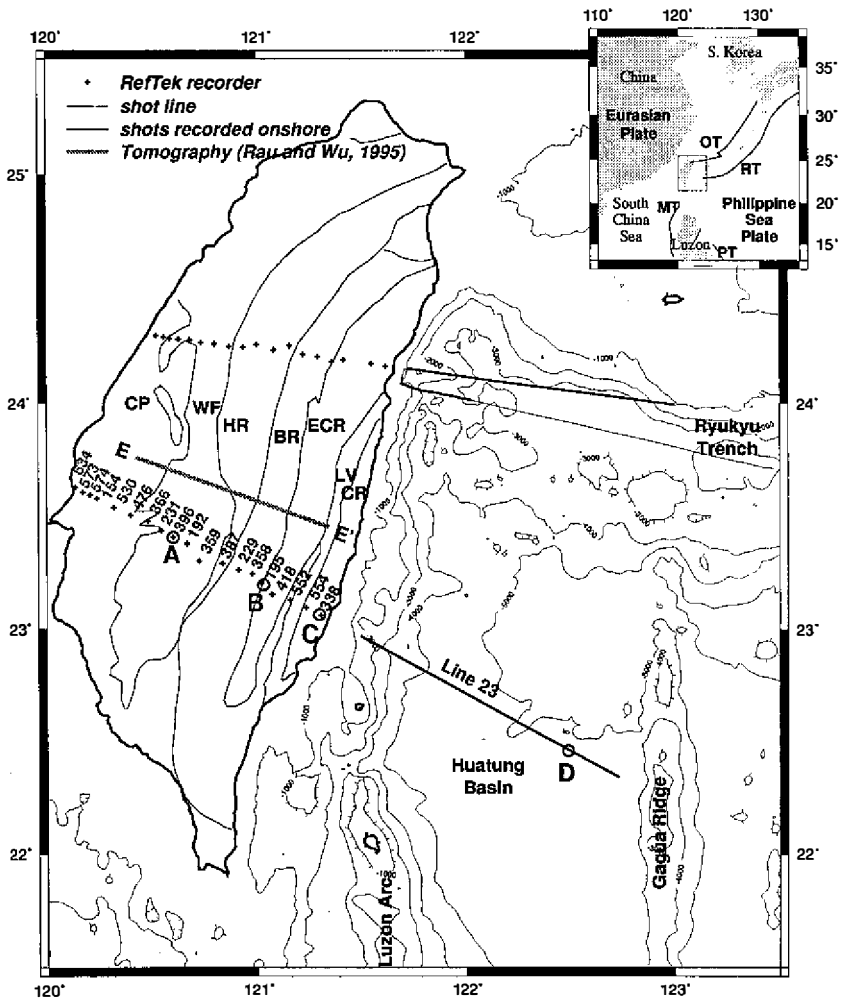

Fig. 1. Locations of transects offshore and onshore of Taiwan. Bathymetry is contoured every 1000 meters and general geological regions are indicated, CP: Coastal Plain, WF: Western Foothills, HR: Hsuehshan Range, BR: Backbone Range, ECR: Eastern Central Range, LV: Longitudinal Valley and CR: Coastal Range. Only the southern profile is presented in this study. All stations deployed on the onshore extension of Line 23 are labeled with their RefTek serial numbers, and the stations with data used in this study are labeled in solid black numbers. The circles refer to endpoints of cross-sections presented in this study, and profile E-E' is a tomography profile determined by Rau and Wu (1995). Inset shows the location of Taiwan in relation to major tectonic features: RT: Ryukyu Trench, OT: Okinawa Trough, MT: Manila Trench and PT: Philippine Trench.

(Chai, 1972; Biq, 1972; Bowin *et al.*, 1978; Wu, 1978; Angelier *et al.*, 1986; Barrier and Angelier, 1986; Ho, 1986; Huchon *et al.*, 1986). The transition zone here should be representative of the orogen. Unfortunately, at stations in the Coastal Plain, the signals from the airguns did not rise above the noisy background and therefore the root of the Central Range is not well sampled. Although wide-angle reflections can be used for imaging the root, they will be analyzed by us in a subsequent study and are discussed by Yeh *et al.* in this issue.

2. DATA

In planning the 1995 R/V Ewing offshore/onshore study east of Taiwan three MCS/OBS lines were charted, and two of them were placed along the extensions of two land instrument deployments as shown in Figure 1. The onshore lines were constrained by the layout of the highways on the island, and by utilizing two cross-island highways these lines were nearly perpendicular to the structural trend of the island. Although a reversal of the southern line was planned, using airgun shots in the Taiwan Strait, it was canceled due to operational difficulties. Altogether 70 stations were established onshore. The 20 (8470 cu. in.) air-gun array of the R/V Ewing was fired every 40 seconds, while steaming southwest with velocity such that shot points were spaced nominally every 100 m. The onshore stations included 37 three channel RefTek recorders with L-28 sensors (PASSCAL, 1994). In this study, we used the vertical component records from the 19 stations on the southern profile (onshore extension of Line 23; Figures 1, 2).

The signals recorded at stations in the Coastal and the Central Ranges were quite clear for offsets up to about 210 km (shot 1250; see Figure 4a). The signal/noise ratios were generally enhanced when filtered with a two-pass, Butterworth band-pass filter (Figure 3; Oppenheim and Schafer, 1989). To enhance the resolution, all time windows with high noise levels were muted after filtering. For stations in the Western Foothills, the signals were not very obvious on individual traces, but when plotted as a section the waves could be readily traced (Figure 4b). However, for stations in the Coastal Plain area the noise level was usually quite high so that no arrivals could be discerned. It appears that the cultural noise in the Coastal Plain was mainly responsible for this problem. For example at station 231 (we use the serial numbers of the RefTek recorders to denote the stations) in the Coastal Plain, the noise level was generally higher than the signals at a neighboring station (396) on the edge of the Central Range.

In this study, we concentrate on the earliest arriving direct and refracted seismic waves, because in a complex structure, the analysis of later arrivals is made difficult by the possible presence of out-of-plane reflections and refractions. The picking of the arrivals on the section plots is relatively easy (Figures 4, 5). We picked the first arrival times on common receiver gathers (CRG). Based on source and receiver reciprocity (Lay and Wallace, 1995), the CRG are east-looking profiles (i.e. equivalent to a profile with source fixed at the receiver site with stations at larger offset toward the east); common shot gathers (CSG) are west-looking profiles. CRG sections from stations 396 and 387 (in the Central Range; Figure 4) and stations 554 and 338 (in the Coastal Range; Figure 5) are presented as examples.

As in all forward modeling studies, we had to associate the arrivals with particular phases. These are done on the basis of simple crustal structures. Data in the Central Range (stations

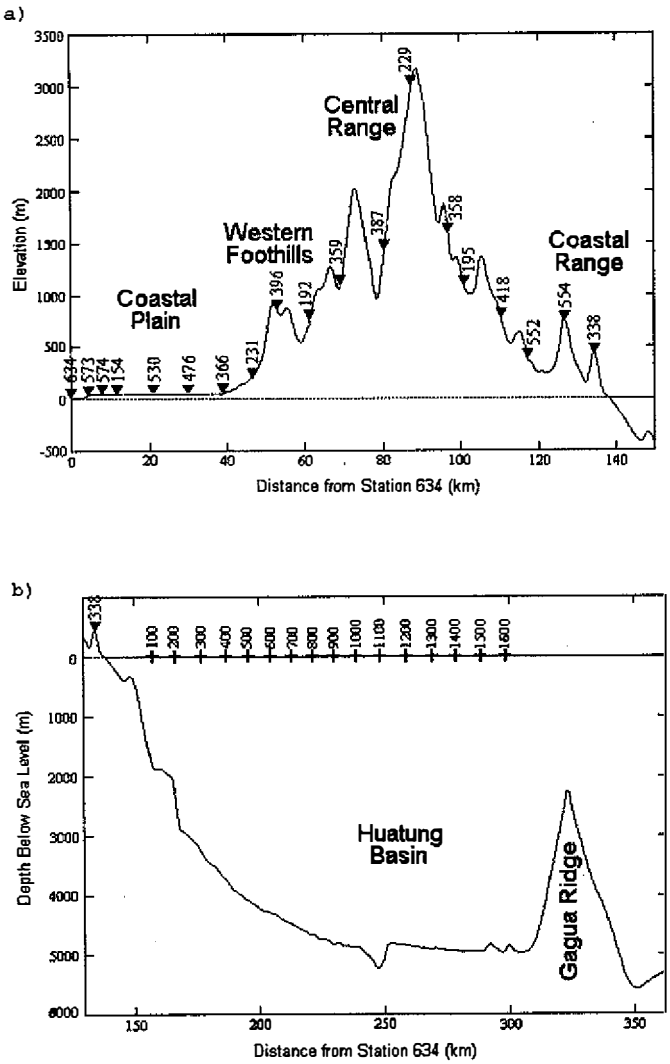

Fig. 2. Offshore-onshore line 23, a) locations of onshore stations (inverted triangles) plotted with elevation of Taiwan, the stations are labeled by their RefTek serial numbers. b) The location of every hundredth shot point (crosses); shots 87 through 1630 were recorded onshore.

396-195) consisted of arrivals which we characterize as refracted P waves in the upper crust (Pg), critically refracted P waves from the Moho (Pn) and P waves refracted in the mantle. However, the arrival times at stations closer to the eastern coast had two additional segments representing waves refracted from mid-crustal velocity discontinuities (Figures 5, 6c-d). On the CRG of stations 418 and 552, there was only one additional segment (Figure 6e), representing a mid-crustal refracted P wave corresponding to the second mid-crustal refracted wave recorded at stations 554 and 338. The apparent velocities (v_a) of the Pg phases on all of the CRG and CSG were approximately 5.5 km/sec. The apparent velocities of the Pn phases on all of the CRG were greater than 8.1 km/sec (at large offsets (>130 km) v_a is as high as 10 km/sec for eastern stations), and were about 6.0 km/sec on the CSG.

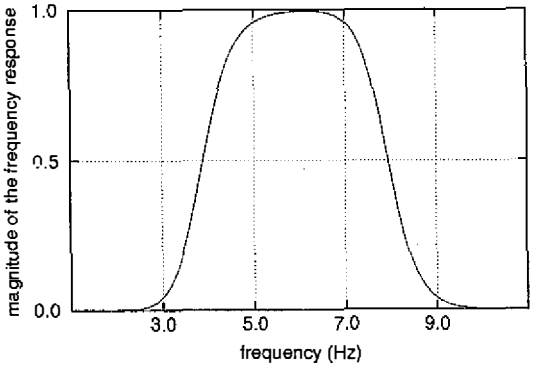

Fig. 3. Magnitude of the frequency response of the Butterworth band-pass filter used in this study. Filter shown was used to filter the data collected by stations 396-552; for brevity, we refer to filter parameters as 3,5-7,9 Hz. We filtered stations 554 and 338 with a Butterworth filter with parameters 4,6-7,9 Hz and 3,5-8,10 Hz respectively. (Oppenheim and Schafer, 1989)

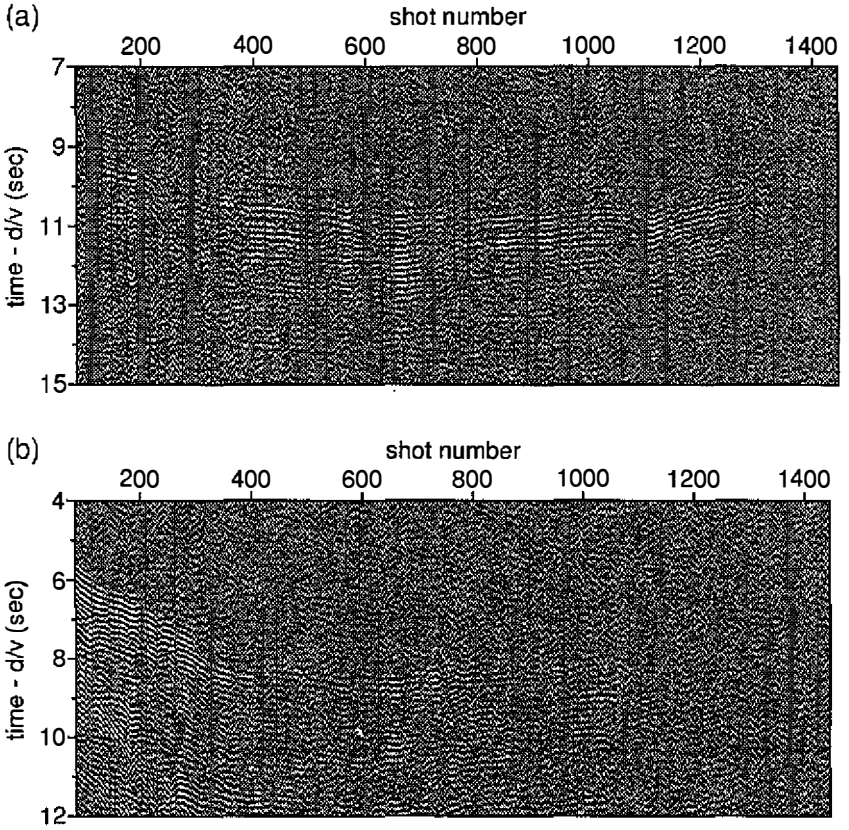

Fig. 4. Common receiver gathers of data collected by two stations, 396 (a) and 387 (b), located in the Central Range, vertical component. Both gathers have been filtered using a two pass Butterworth filter (3,5-7,9 Hz; see Figure 3), and noisy traces have been muted after filtering. Both plots are reduced at 8.1 km/sec.

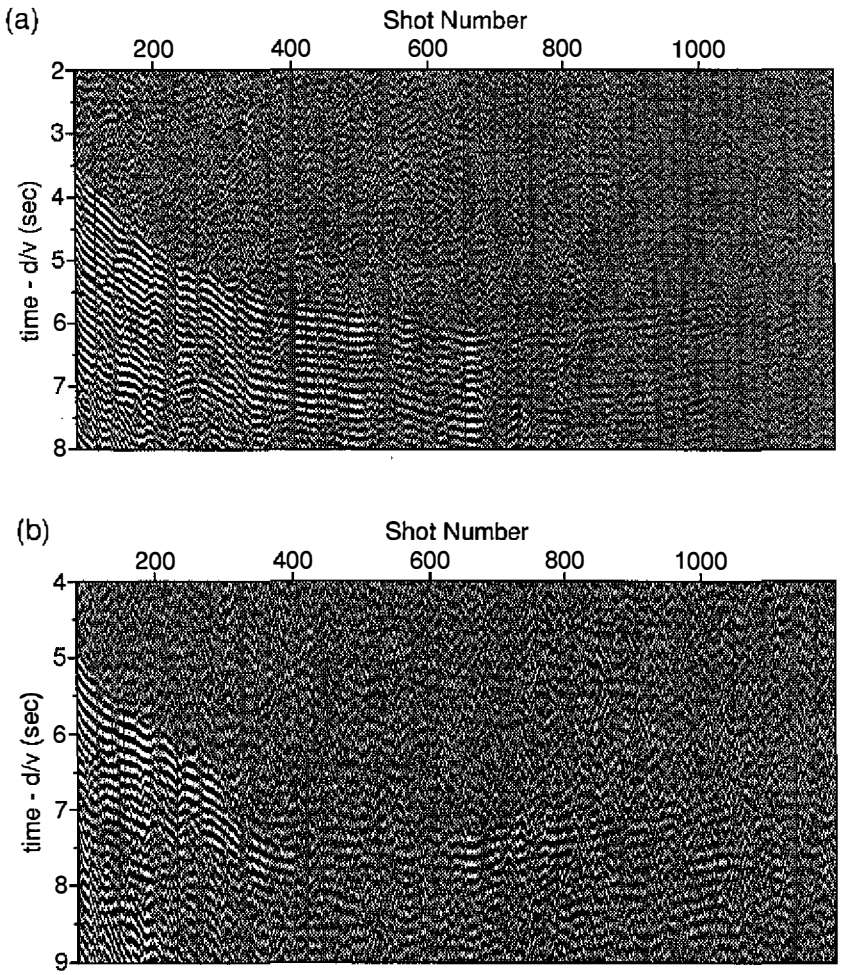

Fig. 5. Common receiver gathers of data collected by two stations located in the Coastal Range, vertical component. Both gathers have been filtered using a two pass Butterworth filter (filter parameters given below; see Figure 3), and noisy traces have been muted after filtering. Both plots are reduced at 7.6 km/sec. a) Station 554, filter parameters: 4,6-7,9 Hz. b) Station 338: filter parameters: 3,5-8,10 Hz.

3. ANALYSES

We relied on forward modeling for this study. Our principle strategy was to start with the simplest layered model that could satisfy the observed data, and fit the calculated arrival times to the observed data with reasonable perturbations of the model. We added structural complexities (i.e., more layers or lateral blocks) to the model, only if the calculated times could not be fitted with minor perturbations of the initial model. Although we could not avoid non-

uniqueness problems, we ensured that the structural complexities added were reasonable. For each velocity model, we calculated travel times using an algorithm adapted from Ocola (1972), which is based on simple geometric ray considerations. We isolated several acceptable models and used the ray tracing package TRAMP (Zelt and Smith, 1992) to determine one average model, which simultaneously modeled the arrivals recorded at all stations. In this paper, we will give enough detail so that the results can be reproduced by other investigators, and naturally, the end product of this study can be further tested with new analysis or when new data becomes available.

We first investigated the general features of the oceanic crust by examining the arrivals recorded at the eastern stations (554 and 338; Figure 5). Based on the apparent velocities on the CRG and CSG, we initially took the oceanic crust structure to consist of three layers (in addition to the water), with velocities in the range of 4.7-5.3, 6.2-6.6 and 6.9-7.7 km/sec, overlying a mantle with velocity of 8.1 km/sec. We made all velocity discontinuities west dipping and planar. The mantle velocity was held fixed throughout all calculations and was based on the OBS analysis by Wang *et al.* (1996). We calculated travel times for the CRG from stations 554 and 338 for over 5000 combinations of boundary depths and dips. We isolated 77 combinations of depths and dips which produced a good least-squares fit of calculated to observed travel times, and then isolated and adjusted the model which achieved the best fit. We also compared the calculated refracted arrivals off the lower mid-crust layer and the Moho to the arrivals recorded at stations 418 and 552. We found that in order to obtain a close fit for stations 418-338, we had to introduce a dip, just east of the coast of Taiwan, on the boundary between the second and third layer (Figure 6). We chose the final velocities to be 5.0, 6.3 and 7.3 km/sec as representative of oceanic crust. However, we could not determine these velocities uniquely with these unidirectional data alone. The first boundary was determined to be 8.5 ± 0.5 km below sea level (b.s.l.) and dipping 0.57 ± 0.25 degrees to the west below station 554. The second boundary was 18.5 ± 1.0 km b.s.l. and dipping 4.6 ± 0.6 degrees to the west below station 554, and 13.3 ± 1.0 km b.s.l. and dipping 2.0 ± 0.6 degrees to the west at 140 km from station 396. We also found that by introducing a gradual increase of dip in the Moho towards Taiwan, we could better model the Pn arrivals recorded at stations 418-338 (Figure 6). However, this gradual dip in Moho was necessitated by analysis of the stations west of the LV.

To constrain the geometry of the Moho, we modeled the Pn and refracted mantle waves recorded at stations in the Central Range. In order to minimize the number of calculations, we chose four stations in the Central Range in the early stages of our study: 396 (Figure 4a) and 192 (referred to in this paper as the western stations) and 387 (Figure 4b) and 358 (central stations). We assumed an average crustal velocity under Taiwan of 6.0 km/sec and a west dipping Moho with mantle velocity of 8.1 km/sec. We calculated travel times for 181 combinations of Moho depth and dip. We found that calculated arrival times of Pn waves for a Moho which fitted the observed data recorded at the central stations (387 and 358) were too slow to fit the western stations (396 and 192; Figure 7a). When we tried to explain this delay by a lower average crustal velocity under the western stations, we found that the average crustal velocity needed to be at least 1.3 km/sec lower, in addition to lowering the Moho velocity to 7.85 km/sec under the island. Since the needed average crustal velocity change is

over a distance of less than 20 km, which is unrealistic, we concluded that the Moho must be increasing dip to the west.

To determine the overall geometry of the Moho, we modeled the Moho as a smooth, continuous function with increasing dip to the west, and approaching horizontal in the Philippine Sea basin. We calculated travel-times for more than 1000 Moho configurations, and iterated the average continental crust velocity from 4.0 km/sec to 6.5 km/sec in steps of 0.5 km/sec. We found that there were several configurations which simultaneously fit the observed data, recorded at the western and central stations (Figure 7b). For a crustal velocity of 6.0 km/sec, the set of acceptable Moho configurations is shown in Figure 8. Quantitatively, at a distance of 100.0 km from station 396 (just off the east coast of Taiwan) the Moho is 28-34 km below sea level (b.s.l.) with a 26-32 degree dip, and 140 km from station 396 the Moho is 19-23 km b.s.l. with a 4-8 degree dip. The effect of changing the average crustal velocity under the Central Range was to shift the function representing the Moho horizontally: a 0.5 km/sec rise shifted the Moho approximately 30 km to the east, while a 0.5 km/sec decrease resulted in a 30 km shift to the west. We chose the average crustal velocity under the orogen of Taiwan to be 6.0 km/sec, which is consistent with the tomography results of Rau and Wu (1995). We selected a particular Moho configuration which lies within the range of possible Moho configurations (Figure 8) whose Pn and refracted mantle arrivals fit data at all of the stations (Figure 9). Obviously, this model is still a generalization, but it shows the overall structures of the crust well.

4. CONCLUSION AND DISCUSSION

We analyzed over 10,000 refracted P wave arrivals (Figures 4,5) from an offshore-onshore seismic experiment. The result of modeling these first arrivals leads us to conclude that under the eastern margin of Taiwan, along the onshore profile across the Southern Cross-Island highway, the crust thickens from the PSP to under the east coast of Taiwan. Although the current data set allows us to resolve only a range of crustal models, there is no question that the dip of the Moho steepens significantly toward the west near Taiwan. Furthermore, this conclusion is supported by the analysis of wide-angle reflections along this same profile by Yeh *et al.* (this issue). The tomographic result of Rau and Wu (1995) and the interpretation of seismicity in terms of the rheology (Wu et. al., 1997) did provide indirect evidence that the oceanic crust must have thickened in the vicinity of Taiwan, but this is the first time such phenomenon is observed directly (Figure 10).

That the crust under the Coastal Range is thickened relative to the adjacent ocean is not surprising. The Coastal Range is composed mainly of trench sediments and island-arc volcanics, evidently a foreshortened oceanic crust (Ho, 1988), with a shortening of perhaps one hundred kilometers. Such shortening would be obviously accompanied by thickening. The mechanism for the thickening is most probably related to thrust-faulting as revealed by recent earthquakes in this region (Salzberg, 1996). With the Coastal Range at an elevation of 1 km, the presence of thickened crust to support it is also reasonable. It is interesting to note that the Bouguer gravity anomaly is positive at nearly 100 mgal at the Coastal Range. This is evidently achieved, despite the thickened crust, by raising higher density oceanic crust to shallow

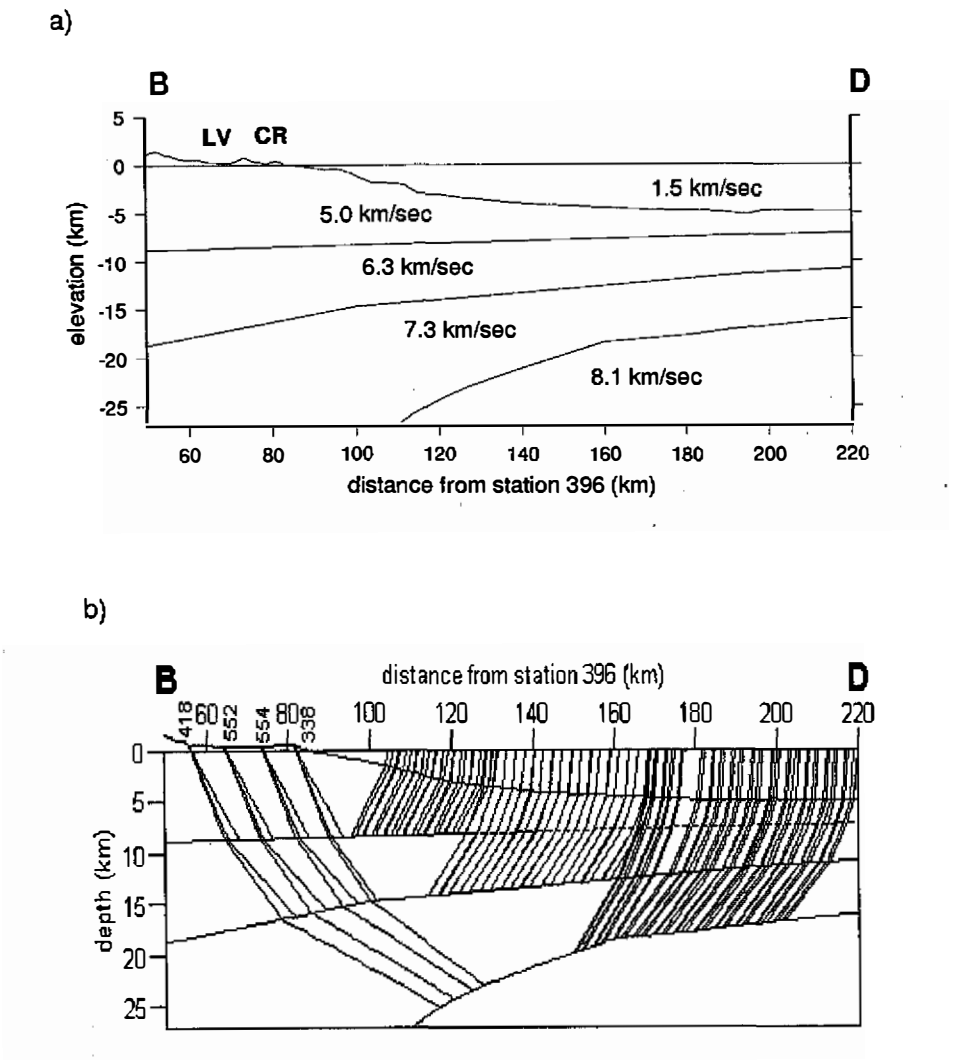

Fig. 6. Cross-section of crustal structure that models the observed arrival times recorded by stations in the Longitudinal Valley and Coastal Range. a) The structure found to model the arrival times for stations 418, 552, 554 and 338. The velocity in each layer is constant. LV is the Longitudinal Valley, and CR is the Coastal Range. b) Ray diagrams for Pn and the head waves off of the two mid-crustal velocity discontinuities for stations 418, 552, 554 and 338 (vertical exaggeration is 2x). Note that shots began to be fired on this line at about 105 km from station 396. Calculated arrival times plotted with data recorded at stations 338 (c), 554 (d) and 552 (e), P1 and P2 refer to the head waves off the first and second mid-crustal boundary respectively.

c)

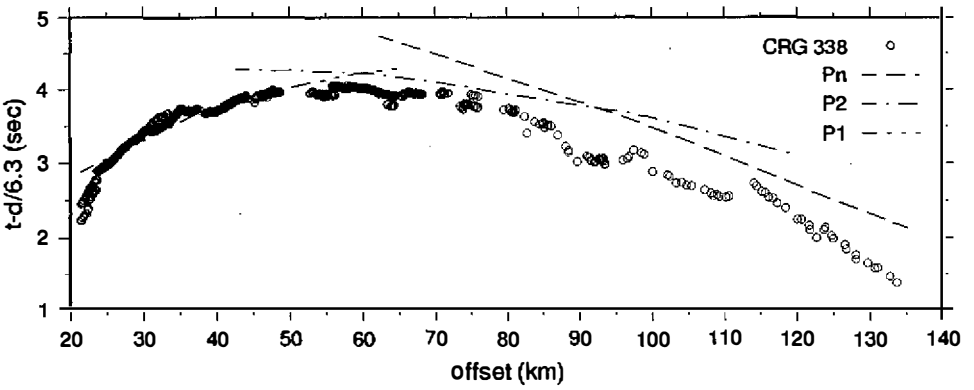

d)

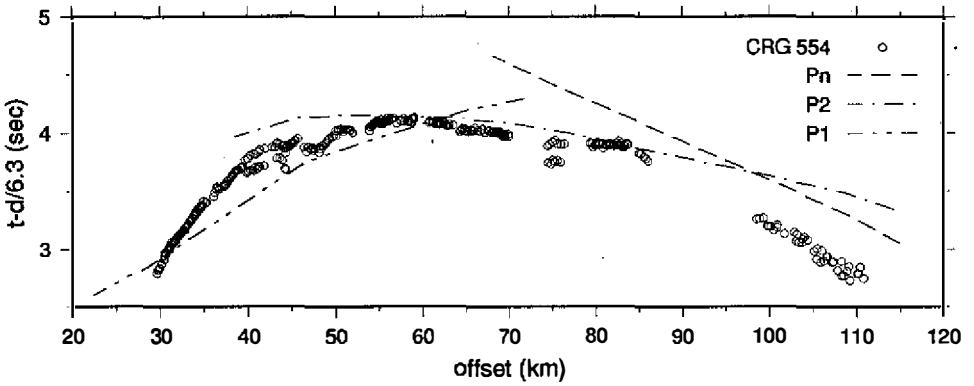

e)

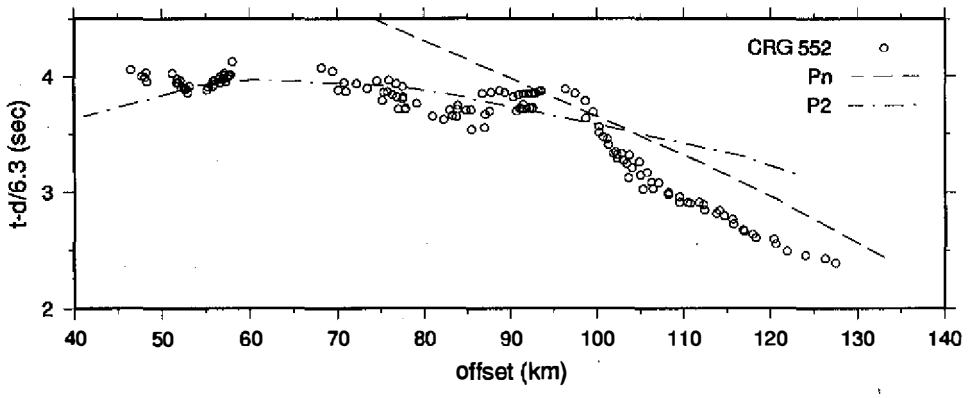

Fig. 6. (continued)

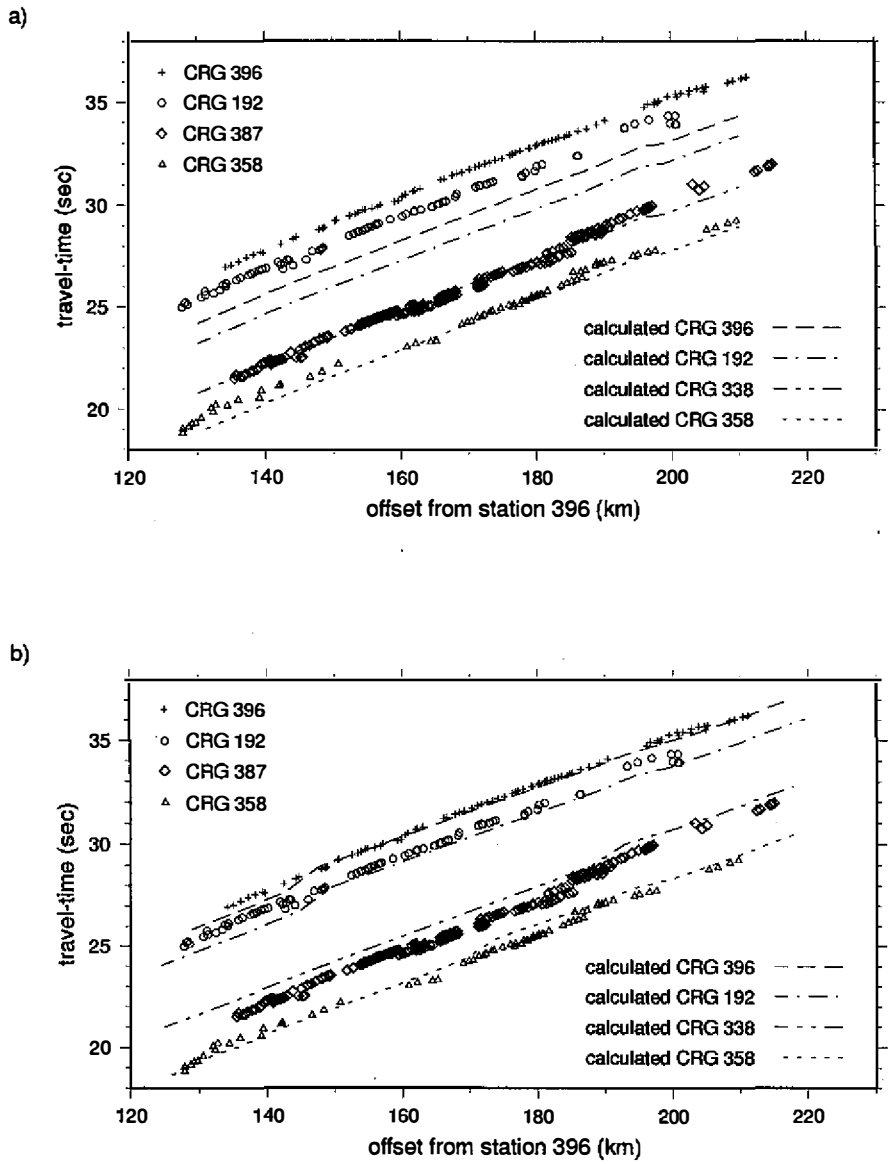

Fig. 7. Calculated and observed arrival times of Pn and mantle refractions recorded by four Central Range stations. a) Pn arrival times calculated for a planar Moho, 26.0 km below station 396 dipping 2.3 degrees to the west. The calculated times fit the observed times recorded at stations 387 and 358, but are faster than the times recorded at stations 396 and 192. b) Pn arrival times calculated for a Moho with dip increasing to the west. The calculated times simultaneously fit the observed times recorded at stations 396, 192, 387 and 358.

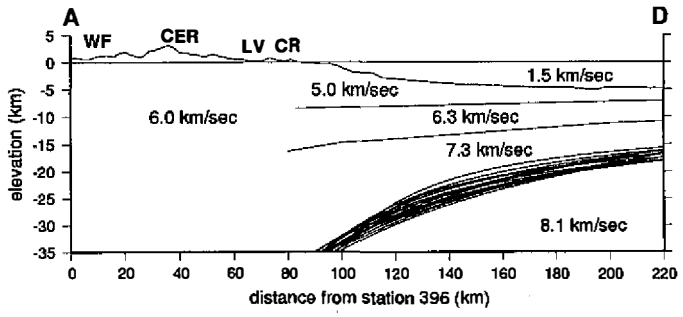

Fig. 8. A suite of Moho profiles that simultaneously model Pn and mantle refractions observed at stations 396-195 (vertical exaggeration is 2x). WF is the Western Foothills, CER is the Central Range, LV is the Longitudinal Valley and CR is the Coastal Range.

a)

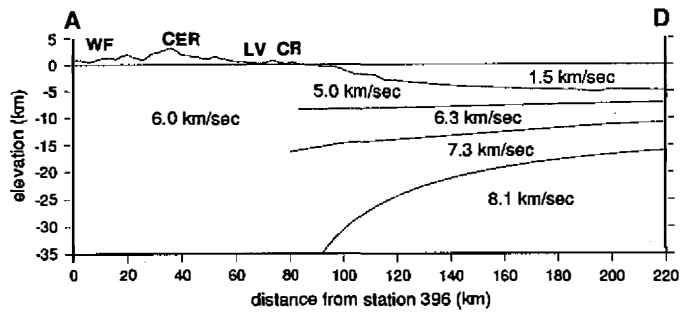

b)

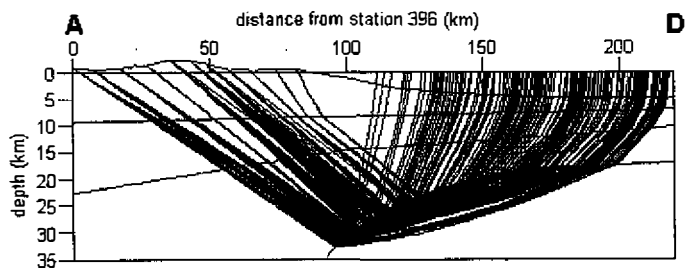

Fig. 9. Velocity model (a) determined from analysis of the first arrival refracted P waves recorded at all stations used in this study, and the ray diagram (b) for Pn and mantle refracted phases (vertical exaggeration is 2x). WF is the Western Foothills, CER is the Central Range, LV is the Longitudinal Valley and CR is the Coastal Range.

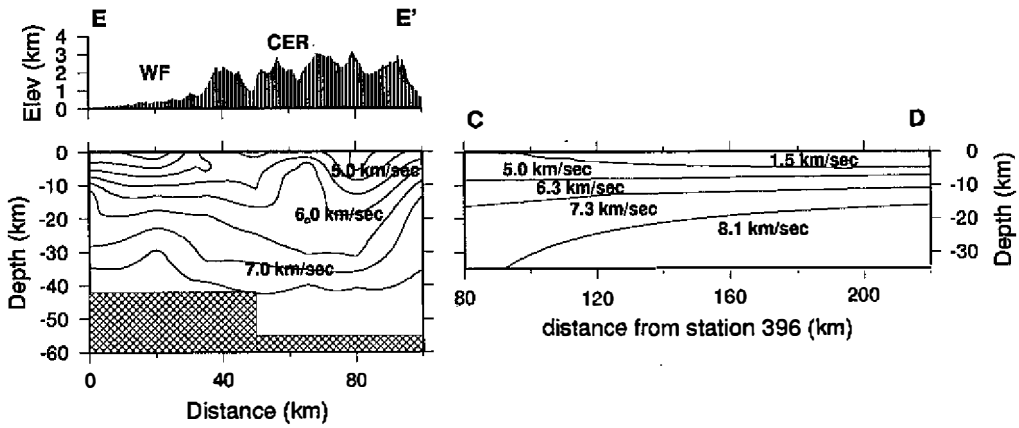

Fig. 10. Comparison of results of this study with the tomography determined by Rau and Wu (1995). See Figure 1 for locations of the cross sections.

depths, similar to what was shown by Wu *et al.* (1997) for the root of the Central Range.

The thickening of PSP is an integral part of the lithospheric collision hypothesis (Wu *et al.*, 1997), and its existence therefore supports the hypothesis. However, by itself, the thickening of the PSP does not argue against the thin-skinned hypothesis, for one can modify it by incorporating a non-rigid indenter. However, the depth at which this thickening occurs is far greater than the depth of the Tertiary sedimentary wedge in question.

The other question one may raise is whether the thickening can be interpreted as westward subduction. Since no other evidence favors the presence of a subduction zone here, crustal thickening alone is not sufficient to argue for it. However, if the underthrusting of denser oceanic lithospheric materials creates an instability, similar to the recognized process of creating a normal subduction zone, then subduction may occur in the future.

Acknowledgements We wish to acknowledge the support of NSF grant INT9513945. The field work was carried out with support from the Institute of Earth Sciences, Academia Sinica, under the leadership of Dr. Y.H. Yeh; in particular, the able group under C.C. Liu lent strong assistance in the field. Dr. R.J. Rau, then at SUNY Binghamton, was responsible for the deployment of our onshore stations. The timely support by the Lamont PASSCAL Instrumentation Center and IRIS/PASSCAL program enabled the onshore recording to be carried out. The planning of the R/V Ewing cruise by Prof. C. S. Liu of the National Taiwan University made the field operation successful. We also thank two anonymous reviewers, Dr. R. Keller and Dr. D. Reed whose keen suggestions and comments greatly improved this manuscript.

REFERENCES

Angelier, J., E. Barrier, and H.T. Chu, 1986: Plate collision and paleostress trajectories in a fold-thrust belt: the Foothills of Taiwan. *Tectonophysics*, **125**, 161-178.

Barrier, E., and J. Angelier, 1986: Active collision in eastern Taiwan: the Coastal Range. *Tectonophysics*, **125**, 39-72.

Biq, C.C., 1972: Dual trench structure in the Taiwan-Luzon region. *Proc. Geol. Soc. China*, **15**, 65-75.

Biq, C., 1981: Collision, Taiwan-style. *Mem. Geol. Soc. China*, **4**, 91-102.

Bowin, C., R.S. Lu, C.S. Lee, and H. Schouten, 1978: Plate convergence and accretion in the Taiwan-Luzon region. *Am. Assoc. Petrol. Geol. Bull.*, **62**, 1645-1672.

Chai, B.H.T., 1972: Structure and tectonic evolution of Taiwan. *Am. J. Sci.*, **272**, 389-422.

Davis, D., J. Suppe, and F.A. Dahlen, 1983: Mechanics of fold-and-thrust belts and accretionary wedges. *J. Geophys. Res.*, **88**, 1153-1172.

Hetland, E.A., and F.T. Wu, 1996: An onshore-offshore seismic reflection profile of Taiwan. *EOS, Trans. Am. Geophys. Un.*, **77**, No. 46, F731.

Hetland, E.A., and F.T. Wu, 1997: An offshore-onshore seismic refraction profile of south-central Taiwan. *Tectonics of East Asia, Programme and Abstracts*, Chungli, Taiwan, R.O.C., 145.

Ho, C.S., 1986: A synthesis of the geological evolution of Taiwan. *Tectonophysics*, **125**, 1-16.

Huchon, P., E. Barrier, J.C. De Bramaecker, and J. Angelier, 1986: Collision and stress trajectories in Taiwan: a finite element model. *Tectonophysics*, **125**, 179-191.

Lay, T., and T.C. Wallace, 1995: Modern global seismology. Academic Press, 517 pp.

Lin, C.H., Y.H. Yeh, B.S. Haung, R.C. Shih, H.L. Lai, C.S. Haung, S.S. Yu, H.Y. Yen, C.S. Lui, and F.T. Wu, 1997: Deep crustal structures inferred from wide-angle seismic data in Taiwan. *Tectonics of East Asia, Programme and Abstracts*, Chungli, Taiwan, R.O.C., 155.

Ocola, L.C., 1972: A nonlinear least-squares method for seismic refraction mapping –Part I: algorithm and procedure. *Geophysics*, **37**, 260-272.

Oppenheim, A.V., and R.W. Schafer, 1989: Discrete-time signal processing. Prentice Hall, 879 pp.

PASSCAL Field Manual, 1994: IRIS, Arlington, VA.

Rau, R.J., and F.T. Wu, 1995: Tomographic imaging of lithospheric structures under Taiwan. *Earth Planet. Sci. Lett.*, **133**, 517-532.

Rau, R.J., 1996: 3-D seismic tomography, focal mechanisms, and Taiwan Orogeny. Ph.D. Thesis, State University of New York at Binghamton, 222pp.

Salzberg, D.H., 1996: Simultaneous inversion of moderate earthquakes using body and surface waves: methodology and applications to the study of the tectonics of Taiwan. Ph.D. Thesis, State University of New York at Binghamton, 272pp.

Shih, R.C., P.J. Chen, C.J. Wu, Y.H. Yeh, C.H. Lin, H.Y. Yeh, and C.S. Lui, 1996: Image of the Taiwan crust from wide-angle and multichannel seismic reflection data. *EOS, Trans. Am. Geophys. Un.*, **77**, No. 46, F731.

Shih, R.C., C.H. Lin, Y.H. Yeh, B.S. Haung, H.Y. Yen, and C.S. Lui, 1997: Stacked images of the deep crustal structure beneath Taiwan from wide-angle seismic reflection data. *Tectonics of East Asia, Programme and Abstracts*, Chungli,Taiwan, R.O.C., 154.

Suppe, J., 1981: Mechanics of mountain building and metamorphism in Taiwan. *Mem. Geol. Soc. China*, **4**, 67-89.

Suppe, J., 1987: The active Taiwan mountain belt. In: J.P. Schaer and J. Rodgers (Editors), The Anatomy of Mountain Ranges. Princeton Univ. Press, pp. 277-293.

Teng, L.S., 1990: Geotectonic evolution of late Cenozoic arc-continent collision in Taiwan. *Tectonophysics*, **183**, 57-76.

Teng, L.S., 1996: Extensional collapse of the northern Taiwan mountain belt. *Geology*, **24**, 949-952.

Wang, T.K., K.D. McIntosh, Y. Nakamura, and C.S. Lui, 1996: OBS refraction survey and imaging offshore eastern Taiwan. *EOS, Trans. Am. Geophys. Un.*, **77**, No. 46, F731.

Wu, F.T., R.J. Rau, and D. Salzberg, 1997: Taiwan orogeny: thin-skinned or lithospheric collision?. *Tectonophysics*, **274**, 191-220.

Wu, F.T., 1978: Recent Tectonics of Taiwan. *J. Phys Earth*, **26**, S265-S299.

Yeh, Y.H., R.C. Shih, C.H. Lin, C.C. Liu, H.Y. Yen, B.S. Huang, C.S. Liu, and F.T. Wu, 1998: Onshore/offshore wide-angle deep seismic profiling in Taiwan. *TAO,* **9**, 301-316.

Zelt, C.A., and R.B. Smith, 1992: Seismic traveltime inversion for 2-D crustal velocity structure. *Geophys. J. Int.*, **108**, 16-34.